

---

Konrad-Zuse-Zentrum für Informationstechnik Berlin  
Heilbronner Str. 10, D-10711 Berlin - Wilmersdorf

Frank Schmidt

Peter Deuffhard

# Discrete Transparent Boundary Conditions for the Numerical Solution of Fresnel's Equation

---

Preprint SC 93-24 (November 1993)

# Discrete Transparent Boundary Conditions for the Numerical Solution of Fresnel's Equation

F. Schmidt, P. Deuffhard

## Abstract

The paper presents a construction scheme of deriving transparent, i. e. reflection-free, boundary conditions for the numerical solution of Fresnel's equation (being formally equivalent to Schrödinger's equation). These boundary conditions appear to be of a nonlocal Cauchy type. As it turns out, each kind of linear implicit discretization induces its own discrete transparent boundary conditions.

**Key words.** Fresnel equation, boundary condition, adaptive Rothe method



## Contents

<b>1</b>	<b>Introduction</b>	<b>1</b>
<b>2</b>	<b>Derivation of transparent boundary conditions</b>	<b>2</b>
2.1	Adaptive Rothe method in the direction of propagation . . . . .	3
2.2	Boundary value problems in the transversal plane . . . . .	4
2.3	Recursive generation of boundary domain functions . . . . .	7
<b>3</b>	<b>Analysis of the constructed boundary conditions</b>	<b>9</b>
3.1	Plane wave solution . . . . .	9
3.2	Uniform mesh and constant coefficients . . . . .	10
3.3	Conservation of energy . . . . .	15
<b>4</b>	<b>Numerical realization</b>	<b>18</b>
<b>5</b>	<b>Application</b>	<b>23</b>



# 1 Introduction

Fresnel's equation, which is formally equivalent to Schrödinger's equation, plays an essential role in such fields of natural sciences and techniques, where wave propagations are considered, e. g., in optics, acoustics and quantum mechanics. The general task in computing a solution of Fresnel's equation is the following: one or more sources are given, which generate waves travelling through the domain of interest and leave it afterwards. In order to simulate the wave propagation, we have to cut out a finite piece of the real problem containing the domain of interest. This paper deals with the choice of the boundary conditions in 2-D problems along our artificially chosen boundaries. We want to realize reflection-free or, equivalently, transparent boundaries, which means boundary conditions so that scattered parts of the wave travelling in the inner region and hitting the boundaries are not reflected in any way back into the interior domain. We want that the boundary conditions realize transparent boundaries for arbitrarily shaped waves going from the inner region to the outer region and vice versa. The problem of the choice of appropriate boundary conditions in the field of wave propagation has been known for a long time and a number of different suggestions have been made. One proposal is to introduce additional absorbing boundary layers next to the simulation domain [7]. This method is the one most often used because it is robust and easy to implement. But it makes an artificial change concerning the original problem and contains additional parameters to adjust. The method can be optimized only over a finite spectral range of the propagating waves. Another method uses a local approximation of the solution near the boundaries with the help of plane waves in order to extrapolate the propagation of the wave through the boundary ([9] and [8]). This method gives good results, if the local approximation is satisfactory, otherwise reflections occur. Although both methods not exact solutions the remaining and unwanted reflections can be neglected in many practical cases. But there are a number of important applications where the results supplied by both methods are not satisfactory even from the practical point of view. Such a situation is given, when scattered waves with a large spectral range (e. g. from an optical grating) hit the boundary. Finishing, a rather new approach, which has to be mentioned, uses a Greens functions representation of the solution in the semi-infinite outer region [1]. This method is superior to the other both from the theoretical as well as from the practical point of view. It gives a true representation of the original problem and very good practical results, if a Green's function representation and a well suited discretization can be found. The method to be discussed in this paper is also a quite general method but does not need any knowledge of Green's function solution of the continuous equation. This means that the method can be applied even in complicated real-life situations where the Green's function is not known. The results presented in this paper lead to a new and efficient algorithm and give new insights into the problem.

## 2 Derivation of transparent boundary conditions

Fresnel's equation in two dimensions is given by

$$(2.1) \quad \begin{aligned} \frac{\partial^2 u(x, z)}{\partial x^2} + \Delta n^2(x, z)u(x, z) &= 2in_0(z)\frac{\partial u(x, z)}{\partial z} \\ \Delta n^2(x, z) &= n^2(x, z) - n_0^2(z) \\ u(x, 0) &= u_0(x), \end{aligned}$$

where  $z$  denotes the direction of propagation,  $x$  the transversal direction,  $n(x, z) \in \mathbf{C}$  the refractive index geometry of the given problem and  $n_0(z) \in \mathbf{C}$  a so called reference index. As Fresnel's equation is used in integrated optics as an approximation of the Helmholtz equation, the reference index  $n_0$  is not given by the physical problem but occurs as a parameter to be adjusted. A useful adjustment of  $n_0$  depends on the solution  $u(x, z)$  itself, therefore  $n_0$  is a function of  $u(x, z)$  in general and is usually not given in advance. However, in our consideration here we do not investigate this nonlinear aspect of the model equation. We assume that  $n_0(z)$  may be given a-priori.

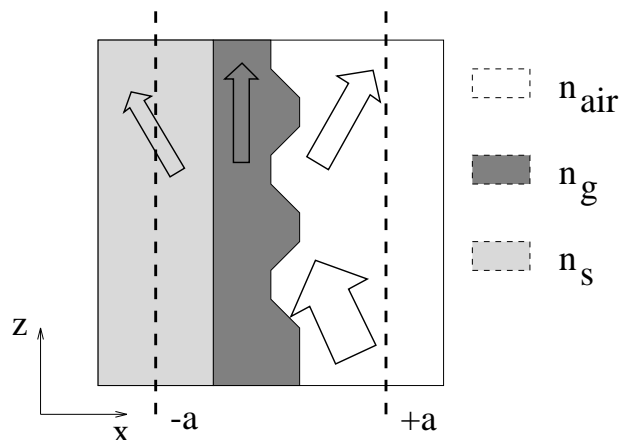


FIG. 1. Schematical drawing of the scattering of an incoming wave on an optical grating. The refractive indexes of the grating  $n_g$ , the substrate  $n_s$ , and the air  $n_{air}$  are constant.

Figure 1 shows a schematic representation of a practical problem. An incoming monochromatic light beam is scattered at an optical surface. The region we are interested in lies between the arbitrarily fixed numerical boundaries  $-a$  and  $+a$ . These boundaries have nothing to do with the physical solution of the problem. If we choose  $n_0 = n_{air}$  in our example, then the  $n^2 - n_0^2$  vanishes in the region to the right of the grating and (2.1) simplifies such that we can easily find a Green's function solution.

But in practice it is found that a sufficient approximation of the wave propagation using Fresnel's equation requires a very careful  $z$ -dependent choice of  $n_\theta$ . Although the  $z$ -dependence of  $n_\theta$  in the given example is weak it has an essential influence on the approximation quality of the *model*. Therefore the usual assumption of a homogeneous exterior domain is not applicable in general.

## 2.1 Adaptive Rothe method in the direction of propagation

We discretize (2.1) first in  $z$ -direction only, using a linear implicit one step discretization. This means, that for an ordinary differential equation (ODE) of the type

$$\frac{du}{dz} = f(u, z)$$

we study the  $\theta$ -family of discretizations

$$\begin{aligned} u_{i+1} - u_i &= \Delta z_{i+1} f(\theta u_{i+1} + (1 - \theta)u_i, z_i + \theta \Delta z_{i+1}) \\ \Delta z_{i+1} &= z_{i+1} - z_i, \end{aligned}$$

for  $\theta$  in the range  $0 < \theta \leq 1$ . When applied to the partial differential equation (PDE) (2.1) we obtain

$$(2.2) \quad \frac{\partial^2 u_{i+1}}{\partial x^2} - \lambda_{i+1}^2 u_{i+1} = -\frac{1 - \theta}{\theta} \frac{\partial^2 u_i}{\partial x^2} + \kappa_{i+1}^2 u_i$$

$$(2.3) \quad \lambda_{i+1}^2(x) = \frac{2in_\theta(z_i + \theta \Delta z_{i+1})}{\theta \Delta z_{i+1}} - \Delta n^2(x, z_i + \theta \Delta z_{i+1})$$

$$(2.4) \quad \kappa_{i+1}^2(x) = -\frac{2in_\theta(z_i + \theta \Delta z_{i+1})}{\theta \Delta z_{i+1}} - \frac{1 - \theta}{\theta} \Delta n^2(x, z_i + \theta \Delta z_{i+1}).$$

Alternatively we introduce the notation

$$(2.5) \quad L_{i+1} u_{i+1} := \frac{\partial^2 u_{i+1}}{\partial x^2} - \lambda_{i+1}^2 u_{i+1}$$

$$(2.6) \quad D_{i+1} u_i := -\frac{1 - \theta}{\theta} \frac{\partial^2 u_i}{\partial x^2} + \kappa_{i+1}^2 u_i,$$

which will be useful when we will consider the discrete Green's function representation of the solution in the exterior domain.

The Rothe-discretization transforms the initial boundary value problem described by the PDE into a boundary value problem described by an ODE of  $u_{i+1}(x)$ . The general solution of (2.2) for arbitrary boundary values is given by

$$(2.7) \quad \begin{aligned} u_{i+1}(x) &= u_1(x) \int_0^x \frac{w_1(\xi)}{w} d\xi + c_+ u_1(x) + \\ &u_2(x) \int_0^x \frac{w_2(\xi)}{w} d\xi + c_- u_2(x), \end{aligned}$$

where  $u_1(x)$  and  $u_2(x)$  are two basis functions  $\in C^2$  which solve the homogeneous part of (2.2)

$$(2.8) \quad L_{i+1}u_{1,2} = 0,$$

and  $w, w_1, w_2$  are the related Wronski determinants

$$w = \begin{vmatrix} u_1 & u_2 \\ \frac{\partial u_1}{\partial x} & \frac{\partial u_2}{\partial x} \end{vmatrix}, \quad w_1 = \begin{vmatrix} 0 & u_2 \\ D_{i+1}u_i(x) & \frac{\partial u_2}{\partial x} \end{vmatrix}, \quad w_2 = \begin{vmatrix} u_1 & 0 \\ \frac{\partial u_1}{\partial x} & D_{i+1}u_i(x) \end{vmatrix}.$$

From (2.2) and (2.8) we find

$$\frac{dw}{dx} = 0$$

and therefore  $w = \text{const.}$

## 2.2 Boundary value problems in the transversal plane

We consider solutions  $u_{i+1}(x)$ , which are quasi exponential bounded in the exterior domain  $|x| \geq a \geq 0$ , i. e.  $u_i(x) \in F_{\gamma,\delta}$  with

$$F_{\gamma,\delta} = \left\{ u_i | u_i \in C^0; |u_i| < K_\gamma e^{\gamma x} \text{ for } x \geq a, \text{ and } |u_i| < K_\delta e^{-\delta x} \text{ for } x \leq -a \right\}.$$

To derive the transparent boundary condition we make a temporary simplification in the notation. We shift the origin of the coordinate system to the right boundary and consider only the exterior domain  $x \geq 0$  (see Fig. 2). The exterior domain is characterized by the fact that the coefficients of (2.1) do not change in x-direction. This guarantees that the exterior domain itself is reflection-free and leads to  $\lambda_{i+1}^2(x) = \lambda_{i+1}^2 = \text{const.}$  In this case (2.7) simplifies to

$$(2.9) \quad u_{i+1}(x) = \frac{1}{2\lambda_{i+1}} \int_0^x D_{i+1}u_i(\xi) e^{\lambda_{i+1}(x-\xi)} d\xi + c_+ e^{\lambda_{i+1}x} - \frac{1}{2\lambda_{i+1}} \int_0^x D_{i+1}u_i(\xi) e^{-\lambda_{i+1}(x-\xi)} d\xi - c_- e^{-\lambda_{i+1}x},$$

where  $\lambda_{i+1}$  is the principal value of the square root of the complex constant  $\lambda_{i+1}^2$ . The unique relation between the two constants  $c_+, c_- \in \mathbf{C}$  and the initial conditions at  $x = 0$  is

$$(2.10) \quad u_{i+1}(0) = c_+ - c_-$$

$$(2.11) \quad \text{and} \quad \left. \frac{\partial u_{i+1}}{\partial x} \right|_{x=0} = \lambda_{i+1}(c_+ + c_-).$$

Now the meaning of (2.9) is the following. If we know  $u_i(x)$  in the boundary domain and assume the constants  $c_+$  and  $c_-$  are given then we can calculate  $u_{i+1}(x)$ . The constants  $c_+$  and  $c_-$  influence the behavior of  $u_{i+1}(x)$  for  $x \rightarrow \infty$  and yield the

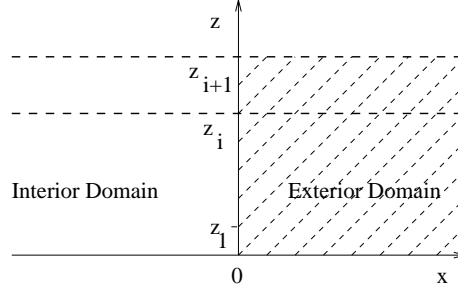


FIG. 2. Separation of the solution and the exterior domain by the boundary at  $x = 0$ . The horizontal dashed lines represent the Rothe discretization method (method of horizontal lines).

boundary conditions for the *inner* solution at the same time. Thus we find that the boundary conditions determine the asymptotic behavior of  $u_{i+1}(x)$ .

To obtain a first formulation of the transparent boundary condition we investigate the asymptotic behavior of the boundary solutions  $u_{i+1}(x)$  generated by source functions  $D_{i+1}u_i(x) \in F_\gamma$  and  $\text{Re}(\lambda_{i+1}) > \gamma \geq -\text{Re}(\lambda_{i+1})$ . In general, (2.9) supplies a quasi exponential bound for  $u_{i+1}$

$$|u_{i+1}(x)| \leq K_1 e^{\gamma x} + K_2 e^{\text{Re}(\lambda_{i+1})x}.$$

Our heuristic to obtain transparent boundary conditions is that this asymptotic behavior of  $u_{i+1}(x)$  should not be influenced by  $\lambda_{i+1}$ , which depends on the chosen  $z$ -discretization. In contrast, it should be determined only by the asymptotic behavior of  $D_{i+1}u_i(x)$ . Consequently, we must determine the constant  $c_+$  such that we have  $K_2 = 0$ . This is realized by

$$(2.12) \quad c_+ = -\frac{1}{2\lambda_{i+1}} \int_0^\infty D_{i+1}u_i(\xi) e^{-\lambda_{i+1}\xi} d\xi.$$

To prove this statement we consider the first two terms on the right hand side of (2.9), which contain the diverging exponential functions and apply (2.12)

$$(2.13) \quad \begin{aligned} & \left| \frac{1}{2\lambda} \left( \int_0^x Du(\xi) e^{-\lambda\xi} d\xi - \int_0^\infty Du(\xi) e^{-\lambda\xi} d\xi \right) \right| |e^{\lambda x}| \\ &= \left| \frac{1}{2\lambda} \left( \int_x^\infty Du(\xi) e^{-\lambda\xi} d\xi \right) \right| |e^{\lambda x}| \\ &\leq \left| \frac{1}{2\lambda} \right| \left( \int_x^\infty K e^{(\gamma - \text{Re}(\lambda))\xi} d\xi \right) e^{\text{Re}(\lambda)x} \\ &= \left| \frac{1}{2\lambda} \right| \frac{K}{\text{Re}(\lambda) - \gamma} e^{\gamma x}. \end{aligned}$$

For completeness we discuss the influence of the remaining two terms in (2.9) on the asymptotic behavior of  $u_{i+1}$ . The absolute value of these terms is less than a quasi exponential bound

$$K_3 e^{\gamma x} + |c_-| e^{-\text{Re}(\lambda_{i+1})x},$$

i. e. that for our restriction the asymptotic behavior again is determined by  $\exp(\gamma x)$ . For  $\gamma < -\text{Re}(\lambda_{i+1})$  the  $\lambda$ -term dominates, in contrast to our heuristic requirement. However, this situation is not critical because by choosing an adequate small stepsize  $\Delta z$  the absolute value of  $\text{Re}(\lambda_{i+1})$  can be made arbitrarily large. Therefore this case is a question of stepsize control.

Now we can give a first formulation of the general transparent boundary conditions. Using the initial conditions (2.10), (2.11), and (2.12) we get

$$(2.14) \quad \left. \frac{\partial u_{i+1}}{\partial x} \right|_{x=0} + \lambda_{i+1} u_{i+1}(0) = - \int_0^\infty D_{i+1} u_i(\xi) e^{-\lambda_{i+1} \xi} d\xi.$$

Equation (2.14) derived for the exterior domain gives an inhomogeneous Cauchy boundary condition for the inner solution too, if continuity of  $u(x)$  and its first derivative can be assumed as it is always the case if the boundary lies in a region of constant coefficients.

Transparency of the boundary conditions means that we can construct boundary conditions which supply the same inner solution like in the case of an infinite exterior domain. We do not want to insert any disturbing effect by our boundary condition. Usually, inadequate boundary conditions give rise to the generation of artificial reflections along the computational boundary.

Next we consider this transparency aspect with regard to our boundary condition (2.14). As the choice of the origin of our coordinate system with respect to  $x$  was arbitrary, any other choice would supply the same form of the boundary condition (2.14), i. e. a shifted coordinate system using  $\bar{x}$ ,  $\bar{\xi}$  such that

$$\bar{x} = x - a, \quad \bar{\xi} = \xi - a$$

with respect to the reference system would supply (2.14) too, with  $\bar{x}$ ,  $\bar{\xi}$  instead of  $x$ ,  $\xi$ . Therefore the appropriate boundary condition at  $x = a$  is

$$(2.15) \quad \left. \frac{\partial u_{i+1}}{\partial x} \right|_{x=a} + \lambda_{i+1} u_{i+1}(a) = - \int_a^\infty D_{i+1} u_i(\xi) e^{-\lambda_{i+1}(\xi-a)} d\xi.$$

The form of the transparent boundary condition (2.14) is translation invariant. To investigate the reflection property of (2.14) it is convenient to restrict to a special set of test functions  $u_{i+1}$ , the plane wave functions with real wavenumbers  $k$

$$(2.16) \quad u_{i+1,k} = e^{ikx}.$$

We consider the test functions  $u_{i+1,k}$  as exact solutions given due to suitable functions  $D_{i+1}u_i$  and appropriate initial conditions at  $x = 0$ . It is  $u_{i+1,k} \in F_0$  therefore the integral representation of  $c_+$  (2.12) exists and can be evaluated. The evaluation of  $u_{i+1,k}$  based on a reflecting boundary condition at  $x = a$  means that at least at one side an additional plane wave with a different wavenumber is generated. However, our transparent boundary condition at  $x = a$  is equivalent to the boundary condition at  $x = 0$ , which was supposed to be right. Therefore an additional generation of reflected waves at  $x = a$  is impossible.

### 2.3 Recursive generation of boundary domain functions

As the determination of  $c_+$  is known by virtue of (2.12), we come back to the general representation of the solution  $u_{i+1}(x)$  in the boundary domain. We rewrite (2.9) together with (2.10) and (2.12):

$$(2.17) \quad \begin{aligned} u_{i+1}(x) &= \frac{1}{\lambda_{i+1}} \int_0^x D_{i+1}u_i(\xi) \sinh(\lambda_{i+1}(x-\xi)) d\xi \\ &\quad - \frac{1}{\lambda_{i+1}} \sinh(\lambda_{i+1}x) \int_0^\infty D_{i+1}u_i(\xi) e^{-\lambda_{i+1}\xi} d\xi \\ &\quad + u_{i+1}(0) e^{-\lambda_{i+1}x}. \end{aligned}$$

The integral terms define a linear operator  $T_{i+1}$  for any  $\text{Re}(\lambda_{i+1}) > \gamma \geq -\text{Re}(\lambda_{i+1})$  and  $f \in F_\gamma$ :

$$(2.18) \quad \begin{aligned} T_{i+1} : \quad &F_\gamma \rightarrow F_\gamma \cap C^2 \\ (T_{i+1}f)(x) &= \frac{1}{\lambda_{i+1}} \int_0^x f(\xi) \sinh(\lambda_{i+1}(x-\xi)) d\xi \\ &\quad - \frac{1}{\lambda_{i+1}} \sinh(\lambda_{i+1}x) \int_0^\infty f(\xi) e^{-\lambda_{i+1}\xi} d\xi. \end{aligned}$$

Equivalently we have for the differential operator defined in (2.6)  $D_{i+2} : C^2 \cap F_\gamma \rightarrow F_\gamma$ , which follows directly from (2.18). Following this process backwards we get  $u_{i+1} \in F_\gamma \cap C^2$  if we have  $D_1u_0 \in F_\gamma$  for the initial field in the exterior domain. As result we obtain a short notation for (2.17)

$$(2.19) \quad u_{i+1}(x) = (T_{i+1}D_{i+1})u_i(x) + u_{i+1}(0)e^{-\lambda_{i+1}x}.$$

Now  $u_i(x)$  itself can be expressed in the same way, and introducing it into (2.19) we get

$$(2.20) \quad \begin{aligned} u_{i+1}(x) &= (T_{i+1}D_{i+1})((T_iD_i)u_{i-1}(x) + u_i(0)e^{-\lambda_i x}) + \\ &\quad + u_{i+1}(0)e^{-\lambda_{i+1}x} \\ &= u_{i+1}(0)e^{-\lambda_{i+1}x} + (T_{i+1}D_{i+1})u_i(0)e^{-\lambda_i x} \\ &\quad + (T_{i+1}D_{i+1})(T_iD_i)u_{i-1}(x). \end{aligned}$$

Finally, the repetition of this process leads to a Green's function representation of the solution  $u_{i+1}(x)$  in the exterior domain

$$(2.21) \quad u_{i+1}(x) = \sum_{j=1}^{i+1} u_j(0)g_{i+1,j}(x) + G_{i+1,0}u_0(x)$$

$$(2.22) \quad \text{with } g_{i+1,j}(x) = (T_{i+1}D_{i+1})(T_iD_i) \dots (T_{j+1}D_{j+1})e^{-\lambda_j x}$$

$$(2.23) \quad \text{and } G_{i+1,0}(x) = (T_{i+1}D_{i+1})(T_iD_i) \dots (T_1D_1).$$

At this stage the transparent boundary condition (2.14) does not appear to be very helpful, because in order to evaluate the boundary condition we have to know the complete solution in the exterior domain of the last z-layer. But this outer solution need not be explicitly computed because we can use a recurrence representation of the integral expression in the right hand side of (2.14). It is convenient to use the following notation for the integral term, where  $\mathcal{L}\{f(x)\}$  is apparently the Laplace transformation:

$$(2.24) \quad F(p) = \mathcal{L}\{f(x)\}(p)$$

$$(2.25) \quad \mathcal{L}\{f(x)\}(p) = \int_0^\infty f(x)e^{-px} dx$$

$$(2.26) \quad p \in \mathbf{C} \quad , \quad f(x) \in F_\gamma, \quad \text{Re}(p) > \gamma.$$

We introduce further the abbreviations

$$(2.27) \quad \Theta = \frac{\theta - 1}{\theta}$$

$$(2.28) \quad \text{and } \sigma_{i+1}^2 = -\left(\Theta\lambda_{i+1}^2 + \kappa_{i+1}^2\right).$$

Now the transparent boundary condition (2.14) reads

$$(2.29) \quad \left. \frac{\partial u_{i+1}}{\partial x} \right|_{x=0} + \lambda_{i+1}u_{i+1}(0) \\ = -\mathcal{L}\{D_{i+1}u_i\}(\lambda_{i+1}) \\ = \sigma_{i+1}^2 U_i(\lambda_{i+1}) + \Theta \left( \left. \frac{\partial u_i}{\partial x} \right|_{x=0} + \lambda_{i+1}u_i(0) \right).$$

In order to construct a recurrence algorithm for  $U_i$  we apply the Laplace transformation to the original discretized equation (2.2) and obtain

$$(2.30) \quad U_{i+1}(p) \left( p^2 - \lambda_{i+1}^2 \right) - pu_{i+1}(0) - \left. \frac{\partial u_{i+1}}{\partial x} \right|_{x=0} = \\ \left( \Theta p^2 + \kappa_{i+1}^2 \right) U_i(p) - \Theta \left( \left. \frac{\partial u_i}{\partial x} \right|_{x=0} + pu_i(0) \right).$$

First we observe that if we choose  $p = \lambda_{i+1}$  equation (2.2) reduces to the transparent boundary condition (2.29). Further, addition of (2.30) and (2.29) yields the desired recurrence formulation:

$$(2.31) \quad U_{i+1}(p) = \frac{u_{i+1}(0) - \Theta u_i(0)}{p + \lambda_{i+1}} + \Theta U_i(p) - \sigma_{i+1}^2 \frac{U_i(p) - U_i(\lambda_{i+1})}{p^2 - \lambda_{i+1}^2}.$$

### 3 Analysis of the constructed boundary conditions

In this section, we now analyze the above derived discrete transparent boundary conditions in the light of a simple model problem - plane waves on uniform meshes for constant coefficients.

#### 3.1 Plane wave solution

Before we proceed further let us consider a simple but informative example. Assume that the coefficients  $n(x, z)$  and  $n_0(z)$  in Fresnel's equation (2.1) are real constants, then (2.1) reduces to

$$(3.32) \quad \frac{\partial^2 u}{\partial x^2} + \Delta n^2 u = 2in_0 \frac{\partial u(x, z)}{\partial z}$$

$$(3.33) \quad \text{with } \Delta n^2 = n^2 - n_0^2$$

$$(3.34) \quad \text{and } \Delta n^2, n_0 \in \mathbf{R}.$$

With a plane wave ansatz

$$(3.35) \quad u(x, z) = e^{-i(\beta z + kx)}$$

$$(3.36) \quad \beta, k \in \mathbf{R}$$

inserted into (3.32) we get

$$(3.37) \quad \Delta n^2 = k^2 + 2n_0\beta,$$

which is called the dispersion relation in optics. Every plane wave (3.35) with wavenumbers  $\beta$  and  $k$  obeying the dispersion relation is a solution of (3.32). Now we use such a plane wave solution with  $\beta, k > 0$  as initial condition at  $z = 0$  and compare the exact solution and the discrete solution according to (2.9) after one z-step at  $z = z_1$ . We contract the inner domain to the boundary itself so we have to deal only with the exterior domains (see Fig. 3).

The initial condition at  $z = 0$  is

$$(3.38) \quad u_0(x) = u(x, 0) = e^{-ikx},$$

and after the first step we have the exact solution

$$(3.39) \quad u(x, z_1) = e^{-i(\beta z_1 + kx)}.$$

The application of (2.17) to the plane wave yield for the right exterior domain

$$u_1(x) = \frac{e^{-\lambda_1 x} (-k^2 \Theta + \kappa_1^2 + u_1(0)(k^2 + \lambda_1^2)) + e^{-ikx} (k^2 \Theta - \kappa_1^2)}{k^2 + \lambda_1^2}.$$

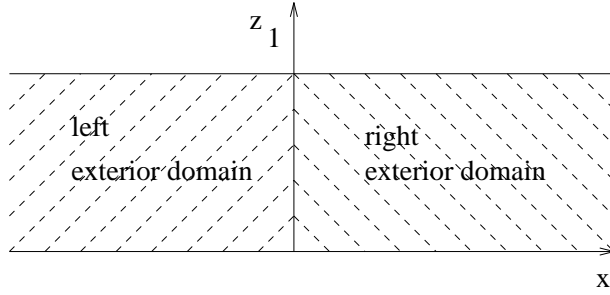


FIG. 3. The inner domain contracts to the boundary itself separating the the semi-infinite left and right outer domains.

The analogous result holds for the left exterior domain ( $\lambda_I$  is replaced by  $-\lambda_I$ ). The continuity of  $u_I(x)$  at  $x = 0$  is realized by construction, the continuity of  $\frac{\partial u_I}{\partial x}$ , which must be fulfilled, leads to

$$u_I(0) = \frac{k^2\Theta - \kappa_I^2}{k^2 + \lambda_I^2}.$$

Therefore we obtain (in consistency with  $u_I(0)$ )

$$u_I(x) = e^{-ikx} \frac{k^2\Theta - \kappa_I^2}{k^2 + \lambda_I^2}.$$

Finally, the insertion of the dispersion relation and the use of the definitions for  $\lambda$  and  $\kappa$  (2.3), (2.4) supplies the desired discrete result

$$(3.40) \quad u_I(x) = e^{-ikx} \frac{1 - i\beta(1 - \theta)z_1}{1 + i\beta\theta z_1}.$$

A comparison of the exact solution and the discrete result shows that we have obtained exactly the solution that we would have obtained by applying our discretization to a first order ODE.

### 3.2 Uniform mesh and constant coefficients

Although the aim of this paper is to give an algorithm for the general case of a nonuniform discretization and  $z$ -dependent coefficients in the outer region the investigation of a uniform  $z$ -discretization with constant coefficients gives some useful insight into the properties of the recurrence formula (2.31). To show, how the evolution of the boundary values  $u_j(0)$ ,  $0 \leq j \leq i$ , influences the boundary condition (2.29) at  $j = i + 1$  we calculate the right hand side of (2.29) as weighted sum of these boundary values. In the

following we assume that  $u_0(x)$  vanishes outside the inner region. Therefore we have  $U_0(p) \equiv 0$ . Due to the uniform discretization we have

$$\lambda_j = \lambda, \quad \kappa_j = \kappa, \quad j = 1 \dots i + 1,$$

which leads to the following form of the transparent boundary condition (2.29)

$$\left. \frac{\partial u_{i+1}}{\partial x} \right|_{x=0} + \lambda u_{i+1}(0) = \sigma^2 U_i(\lambda) + \Theta \left( \left. \frac{\partial u_i}{\partial x} \right|_{x=0} + \lambda u_i(0) \right)$$

A repeated insertion into itself and taking into account that  $U_0$  vanishes yields

$$\left. \frac{\partial u_{i+1}}{\partial x} \right|_{x=0} + \lambda u_{i+1}(0) = \sigma^2 \sum_{j=0}^{i-1} \Theta^j U_{i-j}(\lambda)$$

Due to the Green's functions representation (2.22) we have for the Laplace transform of  $u_m(x)$  at  $p = \lambda$

$$U_m(\lambda) = \sum_{k=1}^m g_{m,k} u_k(0)$$

where the coefficients  $g_{m,k}$  here are the Laplace transforms at  $p = \lambda$  of the appropriate Green's functions  $g_{m,k}(x)$  in space. From this equation we read that it is  $U_m = g_{i,k}$  if  $u_i = \delta_{ik}$  for  $1 \leq i, k \leq m$

$$\begin{aligned} (3.41) \quad \left. \frac{\partial u_{i+1}}{\partial x} \right|_{x=0} + \lambda u_{i+1}(0) &= \sigma^2 \sum_{j=0}^{i-1} \Theta^j \sum_{k=1}^{i-j} g_{i-j,k} u_k(0) \\ &= \sigma^2 \sum_{k=1}^i u_k(0) \sum_{j=0}^{i-k} \Theta^j g_{i-j,k}. \end{aligned}$$

In summary, we obtain

$$\begin{aligned} (3.42) \quad \left. \frac{\partial u_{i+1}}{\partial x} \right|_{x=0} + \lambda u_{i+1}(0) &= \sum_{k=1}^i a_k u_k(0) \\ \text{with } a_k &= \sigma^2 \sum_{j=0}^{i-k} \Theta^j g_{i-j,k} \\ (3.43) \quad &= \sigma^2 \sum_{j=0}^{i-k} \Theta^j g_{i-j-k+1,1}. \end{aligned}$$

The straight forward way to evaluate the coefficients  $a_k$  is to calculate the Laplace transforms of the Green's functions (2.22) and to carry out the summation. Alternatively, we show here how the recurrence formula (2.31) can be used directly to obtain the desired coefficients.

For convenience we introduce the normalized quantities  $\bar{U} = U \cdot \lambda$ ,  $\bar{p} = p/\lambda$ ,  $\bar{\sigma} = \sigma/\lambda$  and drop the bar, which gives the normalized recurrence formula (2.31)

$$(3.44) \quad U_{i+1}(p) = \frac{u_{i+1}(0) - \Theta u_i(0)}{p+1} + \Theta U_i(p) - \sigma^2 \frac{U_i(p) - U_i(1)}{p^2 - 1}.$$

Due to  $u_0(x) \equiv 0$  and  $U_0(p) \equiv 0$  we have for  $i = 0$  immediately

$$(3.45) \quad U_1(p) = \frac{1}{p+1}.$$

To calculate the coefficients  $g_{m,1}$  we consider in correspondence with our discrete Green's function approach (2.21) the recursion of  $U_m(p)$ ,  $1 \leq m \leq i$  for the boundary values  $u_m = \delta_{m,1}$ , i. e. all boundary values for  $m > 1$  vanish. A repeated application of the recurrence formula then leads to

$$(3.46) \quad \begin{aligned} -U_{i+1}(p) \frac{p^2 - 1}{\sigma^2} s^i + g_{i,1}(1) s^i + g_{i-1,1}(1) s^{i-1} + \dots + g_{1,1}(1) s \\ = \frac{\Theta}{\sigma^2} s(p-1) - \frac{p^2 - 1}{\sigma^2} U_1(p), \end{aligned}$$

where the abbreviation

$$(3.47) \quad s = \frac{p^2 - 1}{\Theta p^2 - (\Theta - \sigma^2)}$$

was introduced. If we restrict  $p$  to the principal value and exclude the branch point  $p = 0$ , then there is a unique relation between  $s$  and  $p$  and we can rewrite the right hand side of (3.46) completely in terms of  $s$ . We get

$$\frac{\Theta}{\sigma^2} s(p-1) - \frac{p^2 - 1}{\sigma^2} U_1(p) = \frac{\Theta s - 1}{\sigma^2} \sqrt{\frac{1 - s(\Theta + \sigma^2)}{1 - s\Theta}} - 1 \quad .$$

The right hand side of this equation is expanded at  $s = 0$  into Taylor series with the leading terms

$$\frac{\Theta}{\sigma^2} s(p-1) - \frac{p^2 - 1}{\sigma^2} U_1(p) = \frac{1}{2} s + \frac{\sigma^2}{8} s^2 + \frac{2\Theta\sigma^2 + \sigma^4}{16} s^3 + \dots$$

$U_1(s)$  contains no meromorphic part. As it is clear from the recurrence formula, then all  $U_m(p)$ ,  $m = 1 \dots i+1$  can equivalently be given too in series of  $s$  without a meromorphic part. This enables us to determine all coefficients  $g_{m,1}$  from (3.46) by a comparison of coefficients. We obtain

$$\begin{aligned} g_{1,1} &= \frac{1}{2} \\ g_{2,1} &= \frac{\sigma^2}{8} \\ &\vdots \end{aligned}$$

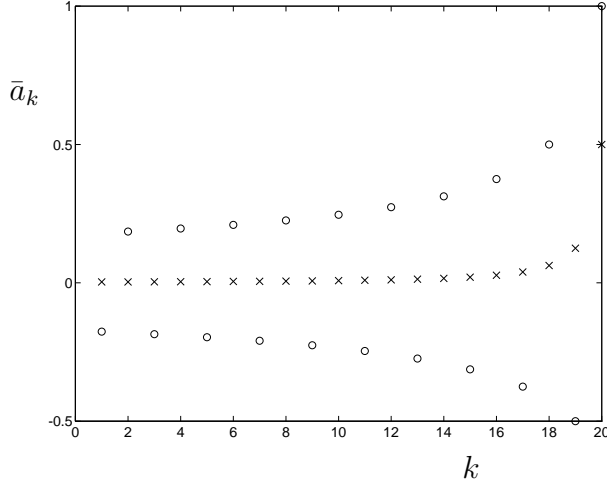


FIG. 4. Normalized weighting coefficients  $\bar{a}_k = a_k/\lambda$ . for the implicit Euler (x) and the implicit midpoint discretization (o) after  $i = 20$  uniform steps have been performed.

It is informative, to specialize this general discretization to the cases of the implicit midpoint and the implicit Euler discretization and to choose  $\Delta n^2 = 0$  in the exterior domain such that we have  $\lambda^2 = -\kappa^2$ . The implicit Euler discretization characterized by

$$\begin{aligned}\theta &= 1, \text{ and therefore } \Theta = 0 \\ \sigma^2 &= \lambda^2,\end{aligned}$$

and the midpoint discretization by

$$\begin{aligned}\theta &= \frac{1}{2}, \text{ and therefore } \Theta = -1 \\ \sigma^2 &= 2\lambda^2.\end{aligned}$$

Taking into account the normalization  $\bar{g}_{m,1} = \lambda g_{m,1}$  we get for the first kind of discretization

$$(3.48) \quad \left. \frac{\partial u_{i+1}}{\partial x} \right|_{x=0} + \lambda u_{i+1}(0) = \lambda \left( u_i - \frac{1}{2}u_{i-1} + \frac{1}{2}u_{i-2} - \frac{3}{8}u_{i-3} + \frac{3}{8}u_{i-4} - \dots \right),$$

and for the latter one

$$(3.49) \quad \left. \frac{\partial u_{i+1}}{\partial x} \right|_{x=0} + \lambda u_{i+1}(0) = \lambda \left( \frac{1}{2}u_i + \frac{1}{8}u_{i-1} + \frac{1}{16}u_{i-2} + \frac{5}{128}u_{i-3} + \frac{7}{256}u_{i-4} - \dots \right).$$

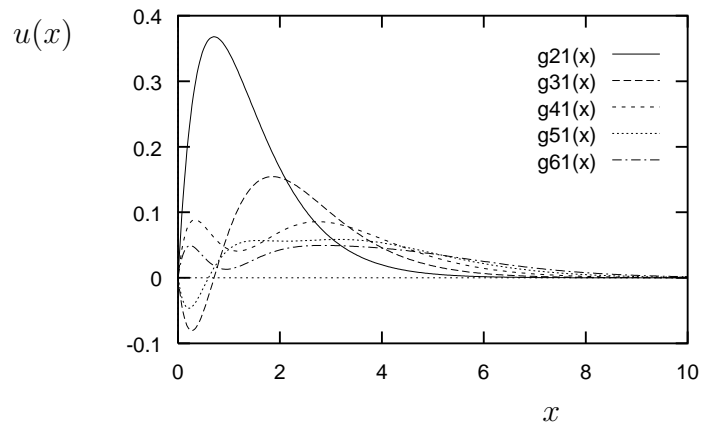


FIG. 5. Green's functions obtained from the implicit midpoint discretization

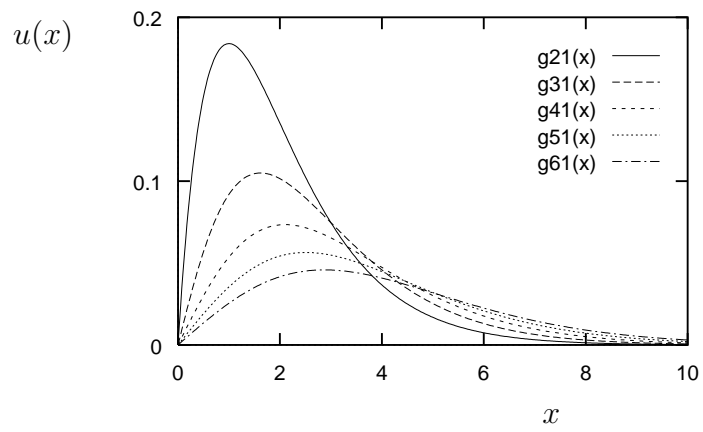


FIG. 6. Green's functions obtained from the implicit Euler discretization

In this notation the nonlocal character of the Cauchy-type transparent boundary conditions is visible. Fig. 4 gives a graphical representation of the normalized coefficients  $a_k/\lambda$ . It becomes apparent that the weights behave very different for different discretizations. This underlines the necessity to construct transparent boundary conditions which fit the discretization scheme as well as aspects related to the continuous equation (e. g. conservation properties). The previous consideration showed that in order to evaluate the transparent boundary condition we do not need an explicit representation of the solutions  $u(x)$  in the exterior domain as it may be expected from the basic recurrence formula (2.29). Further, we have seen that different discretization schemes led to different boundary conditions, and so we expect that the implicit given solutions  $u_j(x)$  in the exterior domain are different too. Therefore we complete the discussion of the uniform discretization case adding the first five functions evaluated using (2.19), starting with  $g_{11} = \exp(x)$ ,  $\lambda = 1$  and assuming  $u_j = 0$ ,  $j > 1$ . Fig. 5 gives the functions  $g_j$ ,  $1 < j \leq 6$  for the implicit midpoint discretization, and Fig. 6 the appropriate curves for the implicit Euler scheme.

### 3.3 Conservation of energy

For practical simulation tasks the conservation of the energy (power) plays an essential role. In Fresnel's approximation we consider the quantity  $p$  as energy

$$p(z) = \int_{-\infty}^{\infty} \overline{u(x, z)} u(x, z) dx.$$

For real constants  $n, \Delta n^2$  the continuous equation (2.1) guarantees

$$\frac{dp}{dz} = 0,$$

if  $u(x), \frac{\partial u}{\partial x} \rightarrow 0$  for  $x \rightarrow \pm\infty$ . It is a natural requirement that in the discrete case the same conservation property should hold. The question arises, what is the influence of the transparent boundary conditions on the evolution of the power in the whole space. Like before, we investigate this question based on the  $z$ -discretized form (2.2) of Fresnel's equation

$$(3.50) \quad L_{i+1}u_{i+1} = D_{i+1}u_i.$$

As now a vanishing field for  $x \rightarrow \pm\infty$  is assumed, we have  $u_i \in F_{\gamma, \delta} \cap C^2$  and  $\delta, \gamma > 0$ . We rewrite the general solution (2.7) by introducing virtual boundaries at  $x = \hat{a}$ ,  $x = -\hat{a}$  with  $\hat{a} \geq a \geq 0$

$$(3.51) \quad \begin{aligned} u_{i+1}(x) = & u_1(x) \int_{\hat{a}}^x \frac{w_1(\xi)}{w} d\xi + c_+ u_1(x) + u_1(x) \int_0^{\hat{a}} \frac{w_1(\xi)}{w} d\xi \\ & u_2(x) \int_{-\hat{a}}^x \frac{w_2(\xi)}{w} d\xi + c_- u_2(x) + u_2(x) \int_0^{-\hat{a}} \frac{w_2(\xi)}{w} d\xi, \end{aligned}$$

Now we let  $\hat{a} \rightarrow \infty$  and insert the transparent boundary conditions instead of  $c_+$ ,  $c_-$  which yields

$$(3.52) \quad u_{i+1}(x) = u_1(x) \int_{-\infty}^x \frac{w_1(\xi)}{w} d\xi + u_2(x) \int_{-\infty}^x \frac{w_2(\xi)}{w} d\xi.$$

This is (of course) nothing else then a generalized version of (2.17). We redefine the operator  $T_{i+1}$  for the whole space  $-\infty \leq x \leq \infty$  and  $\text{Re}(\lambda_{i+1}) > \gamma, \delta \geq -\text{Re}(\lambda_{i+1})$

$$(3.53) \quad \begin{aligned} T_{i+1} : \quad & F_\gamma \rightarrow F_\gamma \cap C^2 \\ (T_{i+1}f)(x) = & u_1(x) \int_{-\infty}^x \frac{-u_2(\xi)f(\xi)}{w} d\xi + u_2(x) \int_{-\infty}^x \frac{u_1(\xi)f(\xi)}{w} d\xi. \end{aligned}$$

In contrast, we have for the differential operators

$$L_{i+1}, D_{i+1} : F_\gamma \cap C^2 \rightarrow F_\gamma$$

and because  $T$  solves (3.50) uniquely to the fixed transparent boundary conditions it is

$$T_{i+1} = L_{i+1}^{-1}.$$

To measure the energy we use the inner product

$$\langle u(x), v(x) \rangle = \int_{-\infty}^{\infty} \overline{u(x)}v(x) dx.$$

The quantity  $\langle u_{i+1}, u_{i+1} \rangle$  should be conserved. If we specialize the z-discretization to  $\theta = 1/2$  (implicit midpoint discretization) we find, see (2.2),

$$D = -\bar{L}.$$

Therefore (3.50) can be written now as

$$\frac{\partial^2 u_{i+1}}{\partial x^2} - \lambda_{i+1}^2 u_{i+1} = -\frac{\partial^2 u_i}{\partial x^2} + \bar{\lambda}_{i+1}^2 u_i.$$

A rearrangement gives

$$\frac{\partial^2(u_{i+1} + u_i)}{\partial x^2} - \text{Re}(\lambda_{i+1}^2)(u_{i+1} + u_i) = i \cdot \text{Im}(\lambda_{i+1}^2)(u_{i+1} - u_i).$$

We calculate the inner product with  $(u_{i+1} + u_i)$

$$\left\langle \frac{\partial^2(u_{i+1} + u_i)}{\partial x^2} - \text{Re}(\lambda_{i+1}^2)(u_{i+1} + u_i), u_{i+1} + u_i \right\rangle = i \left\langle \text{Im}(\lambda_{i+1}^2)(u_{i+1} - u_i), u_{i+1} + u_i \right\rangle.$$

The imaginary part of  $\lambda_{i+1}^2$  do not depend on  $x$  (see (2.2)). Further, as  $u_{i+1}, u_i \in F_{\gamma, \delta} \cap C^2$  and  $L_{i+1}u_{i+1}, L_{i+1}u_i \in F_{\gamma, \delta}$ , we can perform a partial integration with the following result

$$\begin{aligned}
& - \left\langle \frac{\partial(u_{i+1} + u_i)}{\partial x}, \frac{\partial(u_{i+1} + u_i)}{\partial x} \right\rangle - \langle \text{Re}(\lambda_{i+1}^2)(u_{i+1} + u_i), u_{i+1} + u_i \rangle \\
& = i \cdot \text{Im}(\lambda_{i+1}^2) \left( \langle u_{i+1}, u_{i+1} \rangle - \langle u_i, u_i \rangle + \langle u_{i+1}, u_i \rangle - \langle u_i, u_{i+1} \rangle \right).
\end{aligned}$$

Finally, a comparison of the imaginary parts of both sides supplies the desired conservation result

$$(3.54) \quad \langle u_{i+1}, u_{i+1} \rangle = \langle u_i, u_i \rangle.$$

As the conservation of energy is one of the most important questions concerning the wave propagation in integrated optics, we want to investigate the same problem from a slight different point of view. A direct evaluation shows that the operator  $T$  in (3.53) is complex symmetric with respect to our inner product. We find for the adjoint operator  $T^*$

$$T_{i+1}^* = \bar{T}_{i+1} \quad \text{and therefore} \quad L_{i+1}^* = \bar{L}_{i+1}.$$

Now we obtain

$$\begin{aligned}
\langle L_{i+1} u_{i+1}, u_i \rangle &= -\langle \bar{L}_{i+1} u_i, u_i \rangle \\
\langle u_{i+1}, -\bar{L}_{i+1} u_i \rangle &= \langle \bar{L}_{i+1} u_i, u_i \rangle \\
\langle u_{i+1}, L_{i+1} u_{i+1} \rangle &= \langle \bar{L}_{i+1} u_i, u_i \rangle.
\end{aligned}$$

If we compare the imaginary parts of both sides of the last equation we get again (3.54).

## 4 Numerical realization

To realize the transparent boundary condition (2.29) we need as indicated by the recurrence formula (2.31) the numerical value of  $U(\lambda)$  from the step before. There are many different ways to obtain the wanted coefficient. Practical experience showed that a direct numerical approximation of the difference quotient contained in (2.31) tends to instabilities due to the finite computer arithmetic. Therefore we decided to represent  $U(p)$  in fact as a rational function in  $p$  and to carry out a polynomial division. We restrict our consideration to the case of a vanishing outer field  $u_0(x)$  at the initial plane  $z = 0$ , because this is the practically most interesting case. However it does not matter to superpose a nonvanishing initial field if necessary like it is done in (2.21). It has been turned out that the following rational functions supply a useful basis to represent the Laplace transforms  $U_i(p)$  in the Laplace domain

$$q_j(p) = \frac{p - \lambda_j}{p + \lambda_j}.$$

We construct a basis for  $U_i(p)$ , i.e., for the rational polynomials after the  $i$ th step

$$\mathbf{b}^i = \left\{ 1, q_i, q_i q_{i-1}, \dots, \prod_{j=i}^1 q_j \right\}.$$

For a convenient notation we introduce further the abbreviation

$$q_j^i = \prod_{k=i}^j q_k.$$

Now we can write  $U_i(p)$  as

$$U_i(p) = a_{i+1}^i + \sum_{j=i}^1 a_j^i q_j^i.$$

The superscript  $i$  of the complex constants  $a_j^i$  counts the number of steps performed and the subscript  $j$  gives the number of the coefficient in our rational basis.

As pointed out we have for both kinds of discretization

$$\begin{aligned} u(x, 0) = u_0(x) &= 0, \quad x \geq 0 \\ U_0(p) &\equiv 0 \\ \text{and therefore } U_1(p) &= \frac{u_1(0)}{2\lambda_1} (1 - q_1). \end{aligned} \tag{4.55}$$

We assume that  $i$  numerical simulation steps have been done and we need the value of  $U_i(\lambda_{i+1})$  for the next step (see (2.29)). The polynomial  $U_{i-1}(p)$  known from the step before has to be updated to  $U_i(p)$  according to (2.31) and then evaluated at  $p = \lambda_{i+1}$ .

We consider the following recurrence formula which holds for both kinds of discretizations.

$$(4.56) \quad U_i(p) = \frac{u_i(0) - \Theta u_{i-1}(0)}{2\lambda_i} (1 - q_i) + \Theta U_{i-1}(p) + \frac{\sigma_i^2}{4\lambda_i^2} \left( 2 - q_i - \frac{1}{q_i} \right) (U_{i-1}(p) - U_{i-1}(\lambda_i)) .$$

The main difficulty in carrying out this recursion is to find a suitable technique to express the quotient term

$$\frac{1}{q_i(p)} (U_{i-1}(p) - U_{i-1}(\lambda_i))$$

in the original basis  $\mathbf{b}^{i-1}$ . As the technique we need to do this is exactly the same as we need to transform a rational polynomial given in the basis  $\mathbf{b}^{i-1}$  to a representation in the basis  $\mathbf{b}^i$  we concentrate for the moment only on this aspect. We develop this key part of our algorithm in such a way that adjoint summations can be used as effective summation techniques [4]. By insertion we can prove that the following equation holds

$$(4.57) \quad q_j(p) = q_i(p) (\alpha_j q_j(p) + 1) - \alpha_j$$

$$(4.58) \quad \begin{aligned} \alpha_j &= \frac{\lambda_j - \lambda_i}{\lambda_j + \lambda_i} \\ &= -q_j(\lambda_i). \end{aligned}$$

Now a quotient

$$\frac{U_{i-1}}{q_i} = \frac{a_i^{i-1}}{q_i} + \sum_{j=i-1}^1 a_j^{i-1} \frac{q_j^{i-1}}{q_i}$$

can be expressed as (using  $q_j^{i-1} = q_{j+1}^{i-1} q_j$ )

$$\begin{aligned} \frac{U_{i-1}}{q_i} &= \frac{a_i^{i-1}}{q_i} + \sum_{j=i-1}^1 a_j^{i-1} \frac{q_{j+1}^{i-1} (q_i (\alpha_j q_j + 1) - \alpha_j)}{q_i} \\ &= \frac{a_i^{i-1}}{q_i} + \sum_{j=i-1}^1 \left( a_j^{i-1} (\alpha_j q_j^{i-1} + q_{j+1}^{i-1}) - \alpha_j \frac{a_j^{i-1}}{q_i} \right) . \end{aligned}$$

We resolve this summation from behind, i. e. , from  $j = 1$  and obtain

$$(4.59) \quad \frac{U_{i-1}}{q_i} = \frac{a_i^{i-1} - \alpha_{i-1} \tilde{a}_{i-1}^{i-1}}{q_i} + \sum_{j=i-1}^1 \tilde{a}_j^{i-1} (\alpha_j q_j^{i-1} + q_{j+1}^{i-1}) ,$$

where we have introduced the recursion

$$(4.60) \quad \begin{aligned} \alpha_0 &= 0 \\ \tilde{a}_0^{i-1} &= 0 \\ \tilde{a}_j^{i-1} &= a_j^{i-1} - \alpha_{j-1} \tilde{a}_{j-1}^{i-1} \\ &\text{for } j = 1 \dots i-1 . \end{aligned}$$

The polynomial division gives the residual

$$(4.61) \quad r(\lambda_i) = a_i^{i-1} - \alpha_{i-1} \tilde{a}_{i-1}^{i-1}.$$

Looking at the recursion (4.60) and taking into account (4.58) we find that this residual is nothing else then

$$r(\lambda_i) = U_{i-1}(\lambda_i),$$

evaluated using an adjoint summation technique. Finally we have

$$(4.62) \quad \frac{1}{q_i(p)} (U_{i-1}(p) - U_{i-1}(\lambda_i)) = b_i^{i-1} + \sum_{j=i-1}^1 b_j^{i-1} q_j^{i-1}$$

$$(4.63) \quad b_j^{i-1} = \tilde{a}_j^{i-1} \alpha_j + \tilde{a}_{j-1}^{i-1} \\ \text{for } j = 1 \dots i-1.$$

The transformation of a rational polynomial from a basis  $\mathbf{b}^{i-1}$  to a basis  $\mathbf{b}^i$  goes the same way. The polynomial in  $\mathbf{b}^{i-1}$  is divided by  $q_i(p)$  and represented in  $\mathbf{b}^{i-1}$ . The coefficients of the result are the wanted coefficients, the leading coefficient  $a_{i+1}^i$  is the residual  $r(\lambda_{i+1})$ . For the practical computation we split (4.56) into three parts. The first part is already given in  $\mathbf{b}^i$ , the second is given in  $\mathbf{b}^{i-1}$ , and the third in  $\mathbf{b}^{i-1}/q_i(p)$ . (4.56) is rewritten in

$$(4.64) \quad U_i(p) = \beta(1 - q_i) + \frac{\gamma}{2} q_i (U_{i-1}(p) - U_{i-1}(\lambda_i)) + \\ + \gamma U_{i-1}(\lambda_i) - \gamma_{\Theta} U_{i-1}(p) \\ + \frac{\gamma}{2} \frac{U_{i-1}(p) - U_{i-1}(\lambda_i)}{q_i}$$

$$(4.65) \quad \text{with } \beta = \frac{u_i(0) - \Theta u_{i-1}(0)}{2\lambda_i}$$

$$(4.66) \quad \gamma = -\frac{\sigma_i^2}{2\lambda_i^2}$$

$$(4.67) \quad \gamma_{\Theta} = -\frac{\sigma_i^2}{2\lambda_i^2} - \Theta$$

At last the whole recursion is summarized in a pseudo code notation, which shows that the numerical effort to realize the transparent boundary conditions is small. We assume that  $i$  steps have been performed and we want to update the known rational polynomial  $U_{i-1}(p)$  given by the  $i$  memorized coefficients  $a_j$ ,  $j = 1 \dots i$  to  $U_i(p)$ . We need one additional auxiliary vector  $b_j$ . The other coefficients are only temporary. The code is a direct translation of the equations (4.60), (4.62), and the definitions (4.65)-(4.67).

## Pseudo code

```

 $\alpha_0 = 0;$ 
 $\tilde{a}_0 = 0;$ 
for  $j = 1$  to  $i$  do
     $\tilde{a}_j = a_j - \alpha_{j-1}\tilde{a}_{j-1};$  // polyn. division
     $b_j = \tilde{a}_j\alpha_j + \tilde{a}_{j-1};$  // polyn. division
     $b_j = -\gamma_{\theta}a_j + \frac{\gamma}{2}b_j;$  // add old  $\mathbf{b}^{i-1}$ -part
end for;
 $U_{i-1} = \tilde{a}_i;$ 
 $b_i = b_i + \gamma U_{i-1}$ 
for  $j = 1$  to  $i$  do
     $\tilde{a}_j = b_j - \alpha_{j-1}\tilde{a}_{j-1};$  // polyn. division
     $a_j = \tilde{a}_j\alpha_j + \tilde{a}_{j-1} + \frac{\gamma}{2}a_j;$  // add  $\mathbf{b}^i$ -part
end for;
 $a_{i+1} = \tilde{a}_i + \beta;$ 
 $a_i = a_i - \beta - \frac{\gamma}{2}U_{i-1};$ 

```

The Figures 7 and 8 give an impression how the the coefficients  $a_j^i$  behave with respect to both kinds of discretizations applying uniform  $\Delta z$ -steps. To cover the same  $z$ -discretization we used  $\lambda_j = \lambda = 1$  for the implicit Euler discretization and  $\lambda = \sqrt{2}$  for the implicit midpoint discretization. In the first case we have  $U_{50}(1) = 0.9204$ , which converges to 1.0 for  $i \rightarrow \infty$ , in the latter one we find  $U_{50}(\sqrt{2}) = 0.6674$ , which converges to  $1/\sqrt{2}$  for  $i \rightarrow \infty$ .

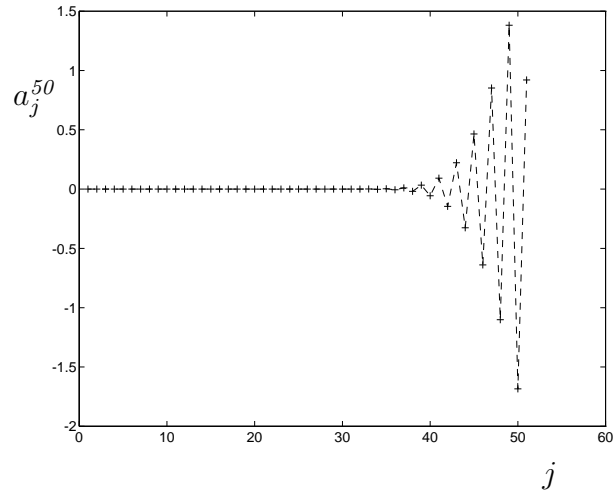


FIG. 7. *Implicit Euler discretization: Polynomial coefficients  $a_j^{50}$  after 50 uniform steps have been performed with  $u_j(0) = 1$  for the whole length.*

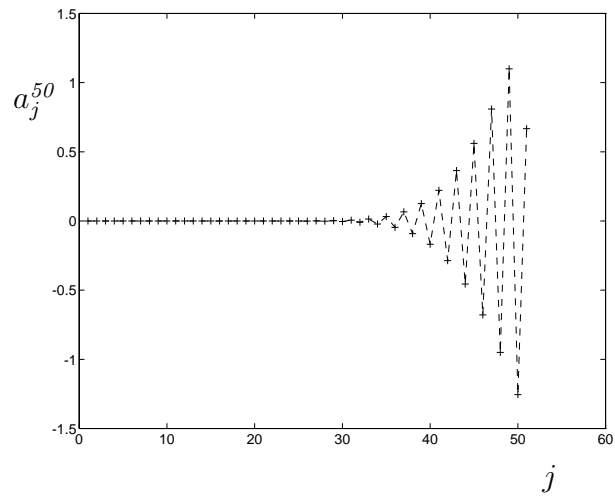


FIG. 8. *Implicit midpoint discretization: Polynomial coefficients  $a_j^{50}$  after 50 uniform steps have been performed with  $u_j(0) = 1$  for the whole length.*

## 5 Application

The transparent boundary conditions were implemented into an existing code which supplies a full adaptive numerical solution of Fresnel's equation both in  $x$  and  $z$ -direction. The transversal field description uses linear finite elements, whereas the  $z$ -discretization was performed applying the implicit midpoint rule. The algorithm of this code called AMIGO1 was developed by one of the authors in [10] for Fresnel's wave equation based on work of Deuffhard et al. [6] and Bornemann [2], [3] for elliptic and parabolic partial differential equations.

All numerical experiments presented in this section are close to real applications. The refractive indexes of the substrates are between 1.5 (glass) and 3.2 (semi conductor). For the light source a wavelength  $\lambda = 1.55\mu m$  was used. Fig. 9 shows the propagation of a Gaussian beam in a homogeneous semi conductor medium tilted with an angle of  $10^\circ$  to the  $z$ -axis. At first we have applied homogeneous Dirichlet boundary conditions. These boundary conditions play the role of metallic walls, i. e., the whole beam is completely reflected. Because the adaptive distributed nodes act as a very sensitive indicator of even weak reflections the related nodes pattern for this and the following experiments are added. By a comparison of this nodes pattern we get an impression how the quality of the transparent boundary conditions influences the numerical effort.

Fig. 10 illustrates this distribution of nodes belonging to the case of zero boundary conditions. Due to the complicated interference pattern of the beam a large number of nodes is necessary to maintain the transversal tolerance below an accepted value. This example demonstrates the trend that reflections may generate a complicated field distribution and therefore lead to a higher density of nodes and so increase the numerical effort. In practice we are often faced with the following situation: The application of nonappropriate boundary conditions results in an incorrect modeling of the real physical behavior and leads to an increasing numerical effort. Therefore the additional effort of the computation of the transparent boundary conditions is in general far less than the gain due to the saved number of nodes and gives an improved problem solution from the physical point of view. Fig. 11 shows the same simulation applying transparent boundary conditions, obtained from the implicit midpoint discretization of the outer domain, and Fig. 12 displays the related distribution of nodes. It can be seen from both results that the evolution of the field is apparently not affected by the artificial boundary. Both simulations were carried out using a tolerance  $TOL_{L_2} = 0.03$  per step, but the CPU times are related as 5:1.

Furthermore, this and all other experiments to discuss in this section serve as examples, in which the reference index and therefore the difference  $\Delta n^2$  are  $z$ -dependent functions in the boundary domain. Fig. 13 illustrates the evolution of the adaptively determined reference index  $n_\theta$  in comparison to the constant substrate index  $n$ . Because the optimal reference index can be seen as the mean phase velocity, it is clear from the physical point of view, that it must converge to the substrate index for  $z \rightarrow \infty$ . In general, the function  $n_\theta(z)$  may have a more complicated behavior, so that a Greens function approach to transparent boundary conditions will be practically impossible for

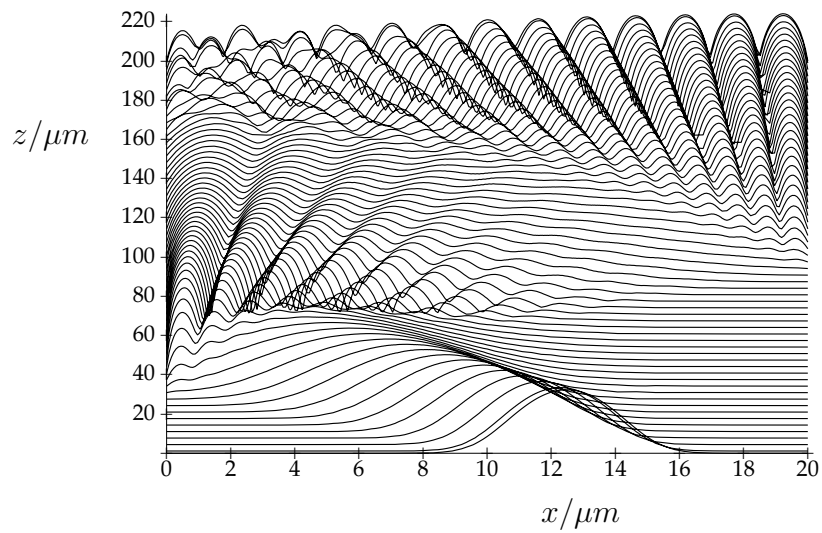


FIG. 9. *Field propagation within metallic boundaries.*

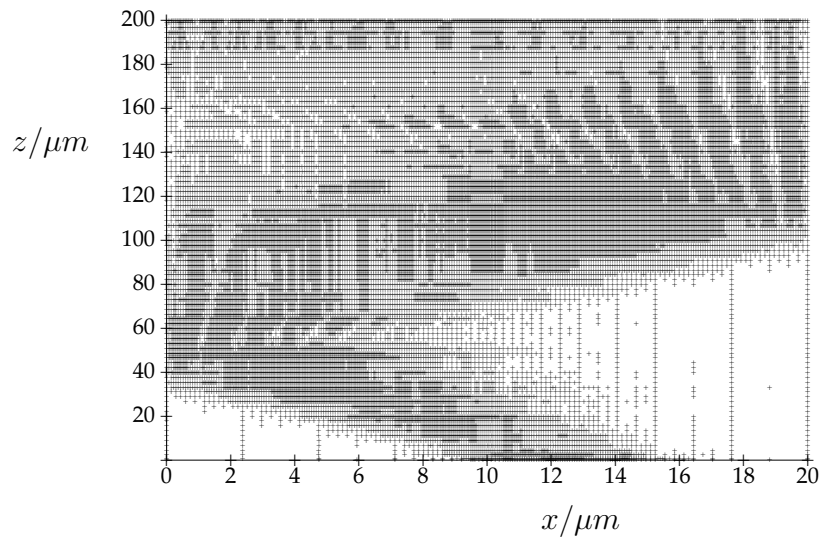


FIG. 10. *Distribution of nodes related to the Fig. 9*

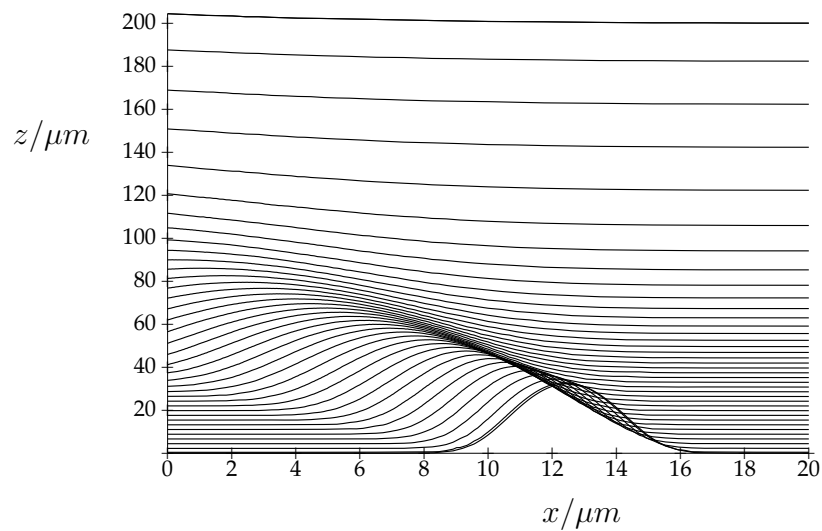


FIG. 11. *Application of transparent boundaries*

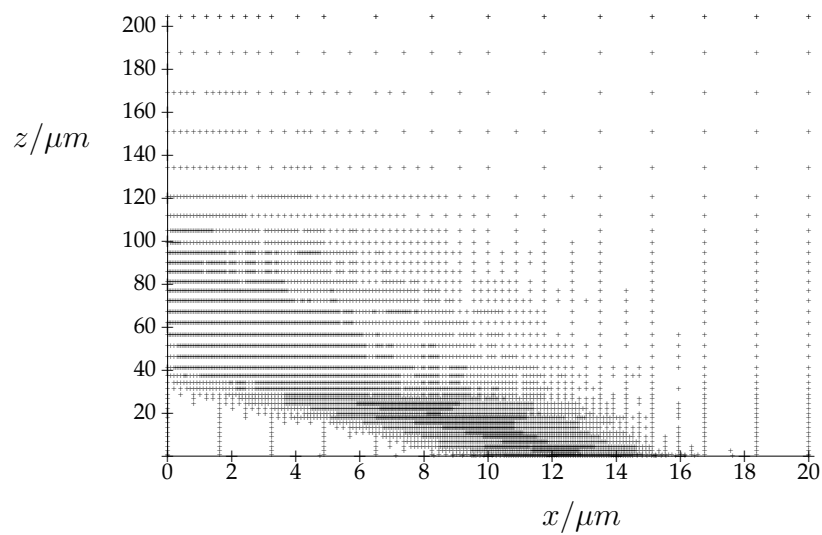


FIG. 12. *Distribution of nodes related to the Fig. 11*

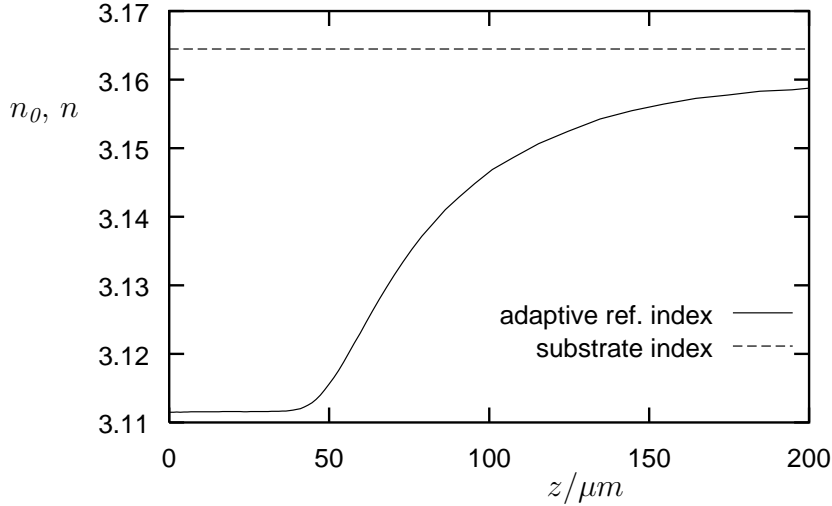


FIG. 13.  $z$ -dependence of the reference index  $n_0$  in comparison to the constant substrate index

such a situation.

To demonstrate what happens if we use the implicit Euler version of our transparent boundary condition instead of the implicit midpoint version, we have performed the same experiment but using the implicit Euler boundary condition. The result is given in Fig. 14. The small difference between both algorithms is sufficient to generate an observable amount of reflections. The practical consequence of such a slight inaccuracy is that considerable more nodes are needed, as it is indicated by Fig. 15.

Fig. 16 shows the evolution of the optical power over the inner cross section  $P(z) = (u(z), u(z))$ , which can be used to quantify the transparency of the boundary condition. As expected, the implicit midpoint version is more transparent than the implicit Euler version because it fits the same kind of discretization as used in the inner domain. However, the power difference at the end is small (less than 1 per cent). If we tight up the tolerance requirement, both curves converge to each other. The advantage in using the implicit midpoint boundary condition is that it supplies the transparency of the boundary even for rough discretizations.

The next experiment models a situation, where the substrate index itself changes abruptly (in  $z$ -direction). Fig. 17 shows the refraction of a Gaussian beam at the interface between a semi conductor medium and glass in a wide computational window. The related result using a small window and transparent boundary conditions is given in Fig. 18. It is seen that the field evolution in this smaller window remains unaffected by the boundary.

Fig. 19 displays the evolution of the reference index  $n_0$  and the substrate index  $n$  belonging to the refraction experiment. As expected, even this large change in the coefficients are covered by the algorithm, because we do not have used any assumption on the refractive index in the outer domain, except it must be independent from the transversal direction  $x$ .

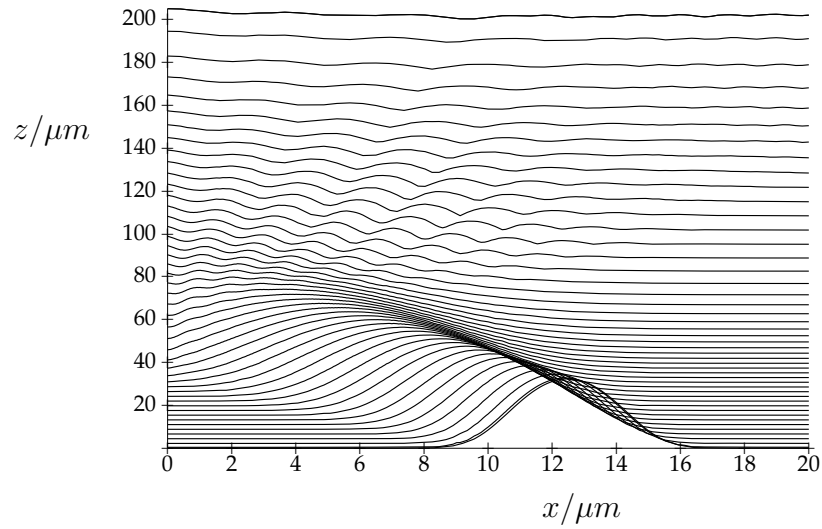


FIG. 14. Application of transparent boundaries using the implicit Euler kind realization of the boundary conditions. Due to the different discretization of the inner and the outer domain reflections occur.

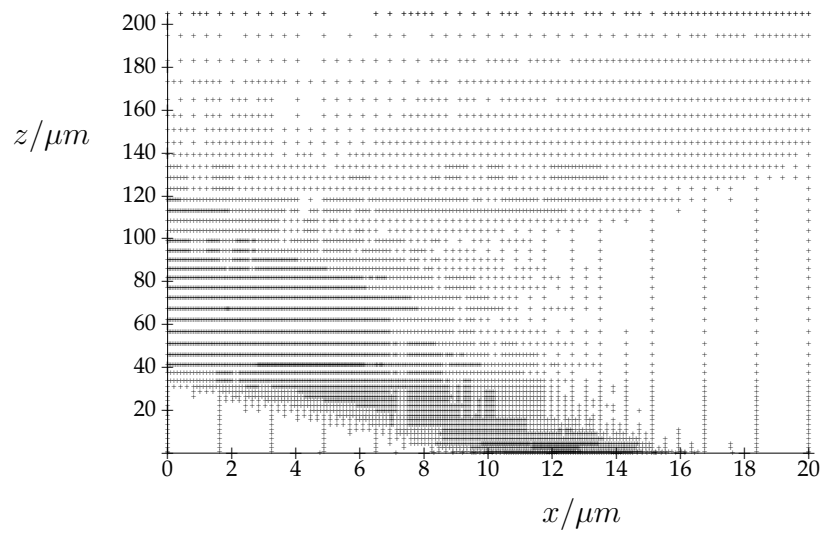


FIG. 15. Distribution of nodes related to Fig. 14. Nodes from reflected modes can be observed.

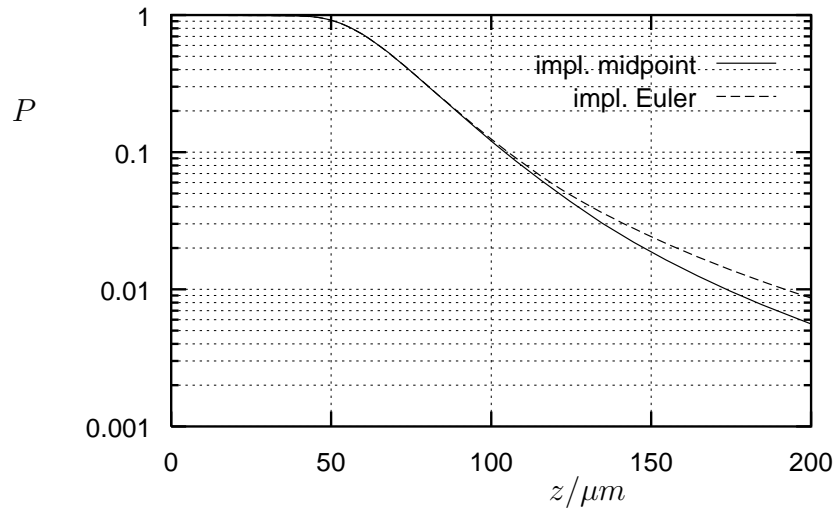


FIG. 16. *Evolution of the power  $P$  contained in the inner domain*

The last experiment concerns the beam interference shown in Fig. 20. Two Gaussian beams propagating with different angles with respect to the  $z$ -axis cause a well known interference pattern.

The restriction of the simulation to the smaller window and the application of the transparent boundary condition gives the result displayed in Fig. 21. Any detail of the original result over this smaller domain is maintained in this new simulation.

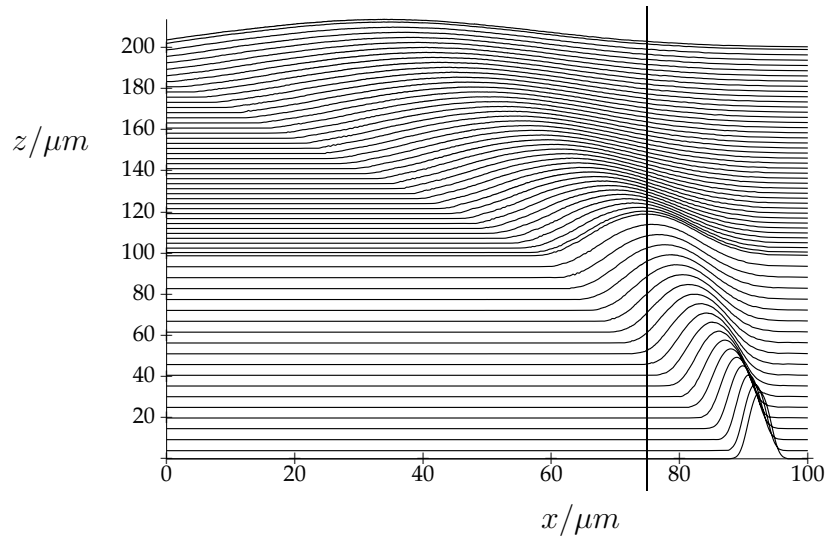


FIG. 17. *Refraction experiment. Two layers of different refractive indexes follow one after the other. The incidence beam is refracted. The line marks the position of the boundary for the following simulation.*

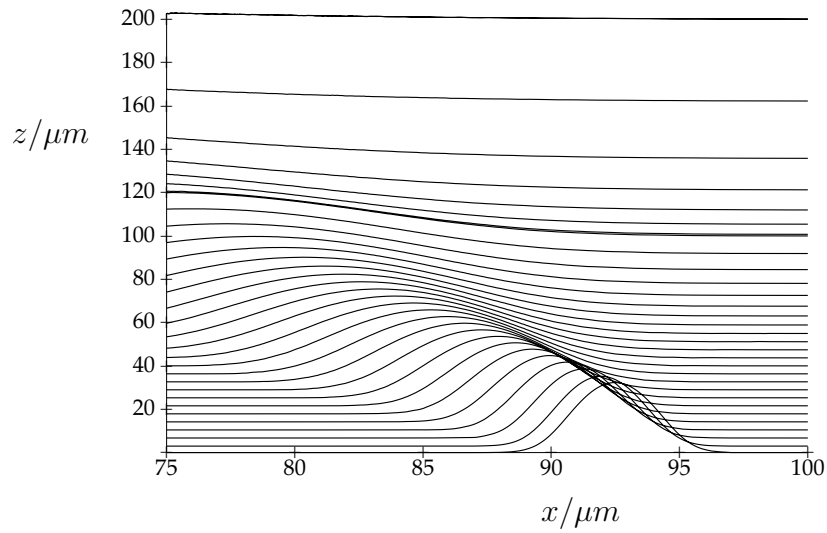


FIG. 18. *The same experiment as before but using a much smaller computational window and transparent boundary conditions.*

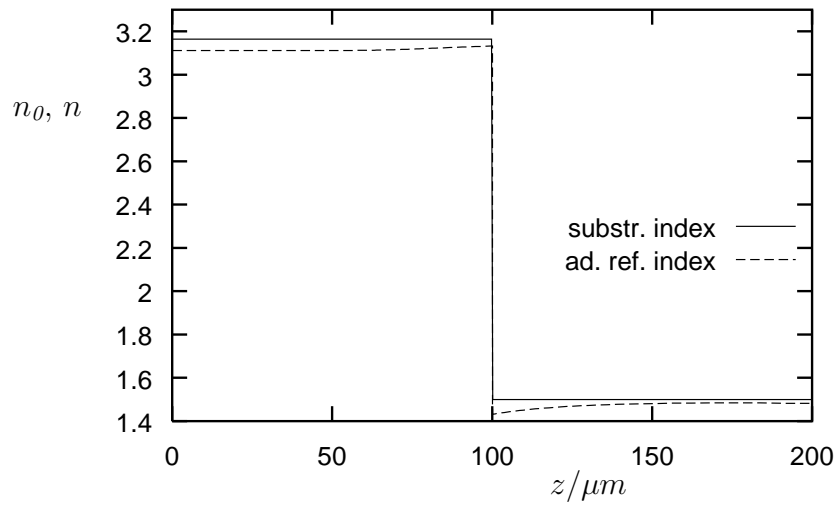


FIG. 19.  $z$ -dependence of the reference index  $n_0$  in comparison to the substrate index. At  $z = 100\mu\text{m}$  the substrate index abruptly changes from  $n = 3.164$  to  $n = 1.5$ .

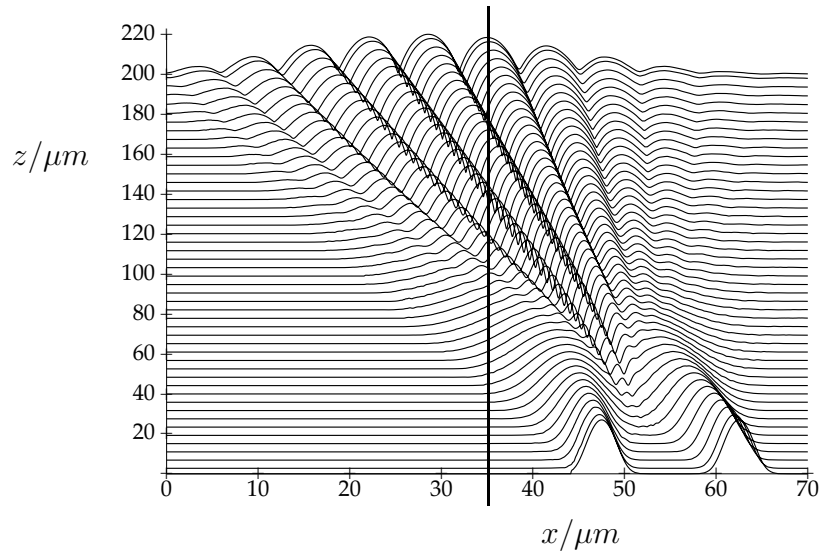


FIG. 20. *Interference experiment. Two Gaussian beams of different incidence angles are superposed and typical interference pattern occur. The line marks the position of the boundary for the following simulation.*

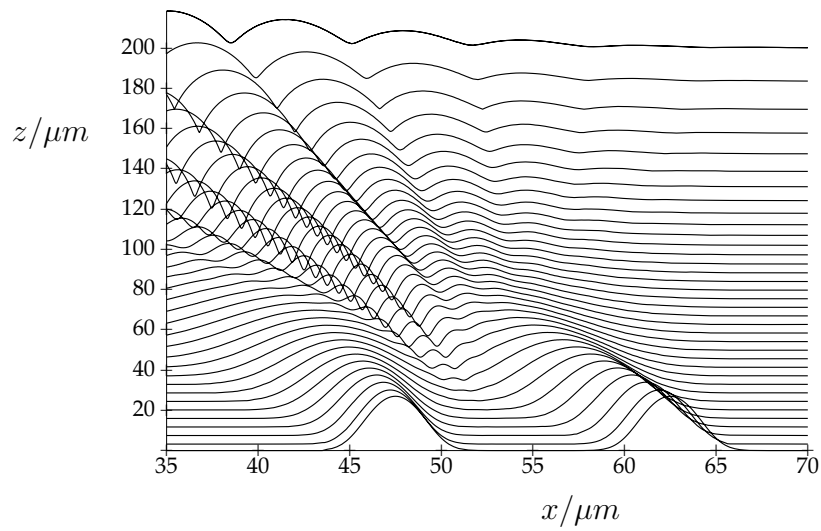


FIG. 21. *The same experiment as before but using a much smaller computational window and transparent boundary conditions.*

## **Conclusion**

We have presented a way of deriving transparent boundary conditions for the implicitly discretized Fresnel's equation. In the opinion of the authors, this way is not restricted only to Fresnel's or equivalently Schrödinger's equation but may be applicable to other linear PDE's describing wave propagation in one way or the other. The transparent boundary conditions appear as nonlocal Cauchy-type boundary conditions. No a-priori knowledge of general solutions in the outer domain in terms of Green's functions is needed, therefore the method can be applied even in the case of nonconstant coefficients. The practical implementation can be performed in form of an recurrence algorithm.

## **Acknowledgment**

The authors thank Dr. F. A. Bornemann, A. Hohmann, Th. Grande (Konrad-Zuse-Zentrum), and Dr. H.-P. Nolting (Heinrich-Hertz-Institut Berlin) for many helpful discussions.

## REFERENCES

- [1] V. A. Baskakov and A. V. Popov: *Implementation of transparent boundaries for numerical solution of the Schrödinger equation* Wave Motion 14, pp. 123-128 (1991)
- [2] F. A. Bornemann: *An Adaptive Multilevel Approach to Parabolic Equations I. General Theory and Implementation.* IMPACT Comput. Sci. Engrg. 2, 279-317 (1990).
- [3] F. A. Bornemann: *An Adaptive Multilevel Approach to Parabolic Equations II. Variable-Order Time Discretization Based on a Multilevel Error Correction.* IMPACT Comput. Sci. Engrg. 3, 93-122 (1991).
- [4] P. Deuffhard: *On Algorithms for the Summation of Certain Special Functions.* Computing 17, pp. 37-48 (1976)
- [5] P. Deuffhard, A. Hohmann: *Numerische Mathematik. Eine algorithmisch orientierte Einführung.* Verlag de Gruyter Berlin, New York (1991)
- [6] P. Deuffhard, P. Leinen, and H. Yserentant: *Concepts of an Adaptive Hierarchical Finite Element Code,* IMPACT Comp. Sci.Eng., 1, pp. 3-35 (1989)
- [7] M. D. Feit, J. A. Fleck: *Light propagation in graded-index optical fibers.* Appl. Optics 17, 3390-3998 (1978).
- [8] G. R. Hadley: *Transparent Boundary Condition for the Beam Propagation Method.* IEEE J. Quantum El. 28, pp.363-370 (1992)
- [9] G. Mur: *Absorbing boundary conditions for the finite-difference approximation of the time-domain electromagnetic-field equations* IEEE Trans. on Elect. Compatibility, EMC-23, pp. 377-382, 1981
- [10] F. Schmidt: *An Adaptive Approach to the Numerical Solution of Fresnel's Wave Equation.* IEEE Journal of Lightwave Technology, Vo. 11 No. 9, pp. 1425-1435 (1993)